NASA TECHNICAL MEMORANDUM

NASA TM X-71866

NASA TM X-71866

(NASA-TM-X-71866) DESCRIPTION OF A COMPUTERIZED METHOD FOR PREDICTING THERMAL FATIGUE LIFE OF METALS (NASA) 15 p HC $3.50 CSCL 11F

N76-18261

Unclas G3/26 18392

DESCRIPTION OF A COMPUTERIZED METHOD FOR PREDICTING THERMAL FATIGUE LIFE OF METALS

by D. A. Spera and E. C. Cox
Lewis Research Center
Cleveland, Ohio 44135

TECHNICAL PAPER presented at
Symposium on Thermal Fatigue of Materials and Components sponsored by the American Society for Testing and Materials
New Orleans, Louisiana, November 17-18, 1975

DESCRIPTION OF A COMPUTERIZED METHOD FOR PREDICTING THERMAL FATIGUE LIFE OF METALS

by D. A. Spera and E. C. Cox

National Aeronautics and Space Administration
Lewis Research Center
Cleveland, Ohio 44135

ABSTRACT

A computer program called "TFLIFE" is described which can be used to predict the thermal fatigue life of metals and structural components from conventional metal properties. This program is used as a subroutine with a main program supplied by the user. The main program calculates input cycles of temperature and total strain for TFLIFE which then calculates a stress cycle, creep and plastic strain damage, and cyclic life. A unique feature of TFLIFE is that it calculates lives according to several different failure criteria for the same input data. These criteria are surface crack initiation, interior crack initiation, and complete fracture of both unnotched and notched fatigue specimens. Sample output tables are shown, together with results for two typical problems: (1) thermal-mechanical fatigue of bar specimens of the tantalum alloy T-111, and (2) thermal-stress fatigue of wedge specimens of the nickel alloy B-1900. Thermal fatigue lives calculated using TFLIFE have been verified by comparison with a variety of laboratory test data on different types of alloys. The computer program is now ready for more extensive evaluation on structural components as well as additional laboratory specimens.

E-8509

INTRODUCTION

This paper describes a fatigue life calculation system utilizing a computer program called "TFLIFE". TFLIFE calculates the low-cycle fatigue life of metals subjected to simultaneous thermal and strain cycling. In conjunction with an elastic structural analysis program, TFLIFE can be used to predict the fatigue life of complete components in high-temperature equipment such as engines and heat exchangers. This paper contains a general description of the program, typical output tables, and results for two sample laboratory test problems.

The original version of TFLIFE was written more than eight years ago to aid in the development of a creep damage theory for thermal fatigue (refs 1 and 2). Since that time it has grown in scope and function, serving as a useful tool for research on high-temperature metals (ref 3). It now includes recent developments in creep-fatigue theory and input/output formats which make it suitable for general use. To date, TFLIFE results have been verified by thermal fatigue tests on laboratory specimens such as bars, tapered disks, wedges, and simulated turbine blades (refs 1-4). In these tests thermal and mechanical loads

were applied by fatigue machines, fluidized beds, and burner rigs to specimens of nickel, iron, cobalt, and tantalum alloys. TFLIFE is now ready for more extensive evaluation by the technical community on complete components as well as laboratory specimens.

A unique feature of TFLIFE is that it calculates thermal fatigue lives according to each of three failure criteria, based on one set of input data. These criteria are (1) surface crack initiation, (2) interior crack initiation (applicable to coated metals) and (3) complete fracture of thermal-mechanical fatigue specimens, both unnotched and notched. Including these three criteria in a single computer program produces a very general and complete analysis of thermal fatigue resistance.

A complete set of the equations used in TFLIFE is given in Ref. 5, together with derivations. Computer time for a typical problem is 8 to 17 seconds on an IBM 360/67 time-sharing system. Required storage capacity is approximately 12000 words.

GENERAL DESCRIPTION OF TFLIFE

Figure 1 is a schematic diagram which describes the general sequence of operations performed by the life calculation system. TFLIFE is a subroutine which is called by a user-supplied main program. This main program, discussed below, contains all calculations of temperature and total strain specific to the specimen or component being analyzed. Initially, the main program calls TFLIFE which reads its own input data (Block I) and divides both the heating and cooling periods into approximately 100 increments. The input data for TFLIFE are of two types: (1) conventional mechanical properties which describe the monotonic tensile and creep-rupture behavior of the metal, and (2) optional empirical constants based on cyclic data. The conventional metal properties must be given for a range of temperatures which includes the thermal cycle being analyzed. The optional empirical constants pertain to cyclic strain hardening, strain concentration, and time-independent fatigue behavior. Nominal values for these constants are contained in TFLIFE for cases in which cyclic data are not available. Input data can be in any of the following three systems of units for stress and temperature: (1) pounds per square inch and Fahrenheit degrees, (2) grams per square millimeter and Celsius degrees, or (3) Newtons per square centimeter and Kelvin degrees. SI (Systeme International) units can be specified for the bulk of the output, irrespective of the input unit system. TFLIFE then returns to the main program.

Temperature, Strain, and Stress Cycles

At Block II in the main program, cycles of temperature and mechanical strain (total strain less free thermal expansion) must be calculated for a potential failure location in the specimen or structure. The complexity of these computations can vary greatly, depending on the structure being analyzed. For a strain-cycled thermal-mechanical fatigue specimen, Block II may only be required to generate saw-tooth or sinusoidal cycles. For a thermal-stress fatigue

specimen it may be necessary to calculate transient temperature distributions and the strains which result from them. In this case a linear elastic analysis is usually sufficient, according to the hypothesis of total strain invariance proposed in Ref 6. This hypothesis states that under conditions of thermal stress, the displacements in a body are substantially independent of local inelastic strains. Thus, displacements obtained by a linear elastic analysis can be used to calculate mechanical strains which can later be divided into elastic, plastic, and creep components. For a complex component it may be necessary for the main program to call a finite-element analysis subroutine. In all cases, a local temperature and a local uniaxial mechanical strain are calculated for each time increment. The system then calls TFLIFE a second time.

In Block III an incremental stress-strain analysis is performed which divides the mechanical strain cycle into elastic, plastic, and creep components. This analysis is repeated until "shakedown" occurs, when the stress-strain hysteresis loop becomes stable and repetitive. In this way a stress, a plastic strain increment, and a creep strain increment are calculated for each time increment. Approximately two-thirds of TFLIFE's computing time is used in these calculations. Upon completion of Block III the mechanical behavior of the material at the potential failure location has been thoroughly described in terms of temperature, stress, and strain. Fatigue damage can now be calculated.

Fatigue Damage and Life Predictions

In Block IV TFLIFE calculates the fraction of the metal's life consumed in one cycle. This calculation uses a fatigue damage model which we call the generalized damage fraction theory (ref 5). The model is so named because it integrates elements from the work of many investigators into a unified, practical method of life analysis. This theory uses Palmgren's linear cumulative damage hypothesis (ref 7) as modified by Taira to include time as a variable (ref 8). Fatigue damage is assumed to to be of two types: (1) elastic-plastic strain damage which is independent of time, and (2) creep strain damage which is time-dependent.

Elastic-plastic strain damage is calculated using an empirical fatigue equation of the exponential type, derived from equations proposed by Basquin (ref 9), Manson (refs 10,11), and Coffin (ref 12). Equations for creep strain damage combine contributions by Robinson (ref 13), Hoffman (ref 14), Taira (ref 8), Swindeman (ref 15), and Spera (refs 1 to 5).

In Block V life predictions are now made for each of the following three failure criteria: (1) surface crack initiation, (2) interior crack initiation, and (3) complete fracture. The first criterion applies mainly to thermal-stress fatigue of an uncoated material. The second criterion can be used to predict the thermal-stress fatigue life of a coated material in which the fatigue life of the coating exceeds that of the substrate material. The third criterion is limited to thermal-mechanical fatigue testing in which strains and temperatures are nominally uniform in the test section of the specimen. The program provides for three strain concentration factors so that the user can

calculate the effect of notch severity on fatigue life. One of these factors is always unity, representing the unnotched condition. The other two factors may be specified arbitrarily by the user or nominal values of 2.0 and 3.0 will be supplied by the program. For notched specimens the input temperature and mechanical strain cycles are considered to be nominal rather than local. Thus five cyclic lives are calculated in Block V for one pair of temperature and mechanical strain cycles as calculated in Block II. This is a unique feature of the TFLIFE computer program.

Output Tables

In Block VI the results of the life analysis are printed in the form of six tables. Samples of some of these tables are shown in Fig. 2 for a thermal-mechanical fatigue problem which will be discussed later. Table 1 (not shown) documents the applied cycle in terms of the mechanical strain range plus temperature, strain, and time limits. Table 2 contains the actual life predictions. These are presented for each of the three failure criteria discussed above. This table also contains damage fractions which show the theoretical proportions of the damage associated with creep strain and elastic-plastic strain for each predicted life. The sum of the two damage fractions is always unity. Also, interior crack initiation and complete fracture are assumed to occur simultaneously in a thermal-mechanical fatigue specimen because of the nominally uniform strain and temperature conditions in the test section.

Table 3 presents temperature, strain, and stress as functions of time during heating and cooling. If the user wishes, this table can be doubled or tripled in length, resulting in smaller time increments and more detailed data on the cycle. Table 4 contains the monotonic tensile data for the material as a function of temperature. This table is constructed from the actual input data using linear interpolation. The number, order, and spacing of temperatures for which property data are given are arbitrary.

The cyclic hardening ratio in the footnote to Table 4 relates cyclic and monotonic stress-strain data. This ratio is an optional scaling factor for proportionately increasing or decreasing yield and ultimate tensile stress values at all temperatures. It is specified by the user according to one of the following three criteria: (1) If no cyclic stress-strain data are available the hardening ratio is unity, which represents neutral hardening. Also, unity is the nominal value used by the program in the absence of a specified value. (2) If partial cyclic stress-strain data are available (for example, at only one temperature) the hardening ratio is adjusted until first-order differences between calculated and observed stresses are eliminated. (3) If complete cyclic stress-strain data are available they are used to calculate equivalent monotonic data for a cyclic hardening ratio of unity.

Table 5 is a summary of the empirical equations which are used in TFLIFE to calculate creep and rupture times (ref 1). The coefficients are calculated from test data by means of regression analysis. Most of the commonly used time-temperature parameters are included in these

general equations as special cases, either exactly or to a close approximation. In this way the equations in Table 5 represent an attempt to select the optimum time-temperature parameter for the available data. If only limited creep rate data are available, simplifying assumptions can be made by the user so that some of the curve-fit constants in the equation for time to one-percent creep are the same as those in the equation for time to rupture.

A final table, Table 6 (not shown), contains data which document the iterations required to acheive convergence. Each iteration is a new calculation of the stress and inelastic strain cycles. The stress at the end of the cooling cycle is carried forward to start the incremental stress analysis for the next iteration. A residual inelastic strain is recorded which is the sum of the plastic and creep strains at the end of each iteration. (Both these quantities are set to zero at the start of each iteration.) A residual inelastic strain of zero represents a completely stable, repetitive stress-strain hysteresis loop. When the residual strain becomes less than 10 micro-units, a curve-fit procedure is used to accelerate convergence, and iteration is terminated after two additional cycles.

Options

After output tables have been printed for one set of input data, there is a minimum of three options which the user can choose to include in the main program: (1) terminating the program, (2) starting the solution to a new problem by reading a new set of data, or (3) varying parameters in the input data which are already stored in the computer and starting the solution to a modified problem. The third option enables the user to perform a parametric study from a single set of input data. As mentioned previously, the operations in the main program are determined by the needs of the user. The TFLIFE system shown schematically in Fig. 1 includes sufficient flexibility to satisfy a wide variety of such needs.

SAMPLE RESULTS

The application of TFLIFE to different types of thermal fatigue conditions will now be illustrated by showing some typical results for the following two problems: (1) thermal-mechanical fatigue of bar specimens of the tantalum-base alloy T-111 tested in vacuum (ref 16), and (2) thermal-stress fatigue of wedge specimens of the nickel-base alloy B-1900 tested in fluidized beds (refs 17,18). Figure 3 shows the geometry of these two types of specimens. The slot notch shown in Fig. 3(b) has a theoretical elastic stress (or strain) concentration factor of 3.0 (ref 19). Predicted lives are given for unnotched and notched bars of T-111 as a function of imposed strain range combined with either isothermal or in-phase thermal cycling. The B-1900 wedge specimen calculations include a study of the effects of changes in cycle time and edge radius for both the uncoated and aluminide-coated conditions of the alloy.

Thermal-Mechanical Fatigue of T-111 Bars

T-111 was selected as a sample alloy because of the variety of thermal-mechanical fatigue data reported on it in Ref 16. Also, its stress-strain behavior is as complex as any which the user is likely to encounter. Therefore, T-111 provides an excellent test of the capabilities of TFLIFE with respect to thermal-mechanical fatigue. The output tables presented in Fig. 2 are taken from one of the T-111 test cases.

Figure 4 shows the simple type of mechanical strain and temperature cycles programmed for these tests. When diametral strain is the control variable, the normal input variable of axial strain is usually unknown prior to the stress analysis (Fig. 1, Block III). TFLIFE resolves this difficulty by using an equivalent axial strain equal to twice the diametral strain plus an equivalent elastic modulus equal to Young's modulus divided by twice Poisson's ratio (ref 5).

Figure 5 illustrates the stress-strain behavior calculated for both the isothermal and in-phase thermal cycles with equal strain ranges. The significantly different shapes of these two calculated hysteresis loops are confirmed by test data (ref 16). Cyclic hardening ratios were selected according to the criteria described previously for cases with partial cyclic stress-strain data (see Output Tables). Two different cyclic hardening ratios were required for these two cycles because the stresses in the in-phase thermal cycle were found to be significantly larger than those in the isothermal cycle for equal strain ranges. A hardening ratio of 1.43 was needed to correlate calculated and observed stresses at point A in the in-phase loop. A much smaller factor, 1.08, matched the calculated stress amplitude in the isothermal loop (point B) to the measured value. These hardening ratios reflect the complex cyclic hardening which has been observed in T-111. For behavior of this type an accurate estimate of the hardening ratio is essential to accuracy in the prediction of creep damage and life.

Figure 6 shows the results of the life calculations for isothermal cycling as a function of axial mechanical strain range. The failure criterion for these tests was complete fracture of the bar specimen. Predicted behavior with a strain concentration factor of unity is in good agreement with the unnotched specimen data, as shown by the open symbols. This correlation between theory and experiment gives a measure a confidence in the extrapolated behavior for lives greater than 1000 cycles. For the notched specimens (closed symbols) predicted behavior is somewhat conservative when the strain concentration factor is equated to its theoretical elastic value of 3.00. The available data were best fit using an empirical strain concentration factor of 2.15. Life predictions based on this factor are given by the dashed line in Fig. 6. In the absence of notched specimen data, the theoretical elastic strain concentration factor would be used as input in TFLIFE.

In Fig. 7 predicted and observed lives are compared for tests with in-phase thermal cycling. Unlike the isothermal tests, the in-phase tests of T-111 showed little notch effect. The TFLIFE predictions are in agreement with the data, whether the strain concentration factor is assumed to be 1.00, 2.15, or 3.00. This insensitivity to strain concentration is related directly to an assumption in the creep damage model in TFLIFE. The assumption is that interior creep damage is not

affected by a surface strain concentration but depends only on the nominal stress. Thus, the strain concentration affects only the elastic-plastic strain component of damage. During in-phase thermal cycling at relatively large strain ranges (lives less than 1000 cycles) most of the damage results from creep (Fig. 2, Table 2). Therefore, the model indicates that strain concentration has only a minor effect on the predicted lives at these strain ranges for in-phase cycling. However, as the strain range decreases below about 0.004, elastic-plastic strain damage becomes dominant over creep damage and a significant notch effect is predicted for this alloy. Figure 7 is an example of an extrapolation of data by TFLIFE that indicates a notch effect at long life which is not present in the short-life data.

Thermal-Stress Fatigue of B-1900 Wedges

Rapid heating and cooling of the wedge specimens shown in Fig. 3 produces edge cracks similar to those often found in turbine blades and vanes. The sequence of calculations required for predicting the initiation period for such cracks is illustrated by the results shown in Figs. 8 to 11. In contrast to the simple cycles shown in Fig. 4, the transient temperature and strain inputs for thermal-stress fatigue problems are quite complex. Consequently, Block II in the main program (Fig. 1) is much more complex for thermal-stress fatigue than for thermal-mechanical fatigue problems. For instance, in this B-1900 problem, thermocouple data taken at several points in the interior of the wedge specimen are curve-fit in Block II for each of the approximately 100 time increments during heating, and the same number of time increments during cooling, as described in Ref 18. These curve-fits are then used to calculate the temperature and mechanical strain cycles at the specimen edges.

Figure 8 shows typical edge temperature transients during heating and cooling. Note that the length of the heating and cooling periods is not sufficient for the temperatures to reach steady-state levels equal to the bed temperatures. In Fig. 9 transient mechanical strain is plotted versus edge temperature rather than versus time. This is often a convenient way to display transient data and to insure that calculated strain and temperature cycles are compatible. Changes during one of the transfer periods are also noted in Figs. 8 and 9, when the specimen is moved from the cooling to the heating bed.

A typical stress-strain hysteresis loop for thermal-stress fatigue is presented in Fig. 10. A cyclic hardening ratio of unity (i.e. neutral hardening) was used to calculate this loop, in the absence of pertinent cyclic stress-strain data. Comparison of Figs. 5 and 10 shows the wide variety of stress-strain behavior possible during thermal fatigue. The hysteresis loop in Fig. 10 has a "figure eight" shape which is produced by changes in elastic modulus with temperature combined with the presence of only small amounts of inelastic strain. The shakedown process during iteration is shown to produce an increase in this cycle's mean stress.

Figure 11 summarizes the dependence of the number of cycles required to initiate edge cracks on the parameters of cycle time and edge radius, for uncoated and aluminide-coated conditions. Comparison

of predicted curves with test data indicate that TFLIFE can correctly model thermal-stress fatigue life on the basis of thermocouple data and monotonic material properties. Furthermore, TFLIFE can be used to predict behavior outside the range of the test parameters.

CONCLUDING REMARKS

The TFLIFE computer program has been found to be a useful tool for analyzing thermal fatigue data in terms of conventional metal properties and for predicting the thermal fatigue life of metals. It contains models for the major damaging phenomena which occur during a general thermal-fatigue cycle, at least to a first-order approximation. Thermal fatigue lives calculated using TFLIFE have been verified by comparison with a variety of laboratory test data on different types of alloys. This computer program is ready for more extensive evaluation by the technical community, not only on additional laboratory specimens but also on structural components.

REFERENCES

1. Spera, D. A., "A Linear Creep Damage Theory for Thermal Fatigue of Materials," Ph.D. thesis, University of Wisconsin, Madison, 1968.

2. Spera, D. A., "Calculation of Thermal-Fatigue Life Based on Accumulated Creep Damage," NASA TN D-5489, National Aeronautics and Space Administration, October 1969.

3. Spera, D. A., and Grisaffe, S. J., "Life Prediction of Turbine Components: On-going Studies at the NASA Lewis Research Center," NASA TM X-2664, National Aeronautics and Space Administration, January 1973.

4. Spera, D. A., "Comparison of Experimental and Theoretical Thermal Fatigue Lives for Five Nickel-Base Alloys," Fatigue at Elevated Temperatures, ASTM STP 520, American Society for Testing and Materials, 1973, pp. 648-657.

5. Spera, D. A., "Equations for Predicting Thermal Fatigue Life," NASA TM (to be published), National Aeronautics and Space Administration.

6. Mendelson, A., and Manson, S. S., "Practical Solution of Plastic Deformation Problems in Elastic-Plastic Range," NACA TN 4088, National Advisory Committee for Aeronautics, September 1957.

7. Palmgren, A., "Die Lebensdauer von Kugellagern," Zeitschrift des Vereines Deutscher Ingenieure, Vol. 68, No. 14, April 1924, pp. 339-341. (English translation, NASA TT F-13460, National Aeronautics and Space Administration, March 1971).

8. Taira, S., in Creep in Structures, N. J. Hoff, ed., Springer Verlag, Berlin, 1962, pp. 96-124.

9. Basquin, O. H., "The Exponential Law of Endurance Tests," Proceedings, American Society for Testing and Materials, Vol. 11, 1910, pp. 625 and 630.

10. Manson, S. S., "Behavior of Materials under Conditions of Thermal Stress," NACA TN-2933, National Advisory Committee for Aeronautics, 1953.

11. Manson, S. S., Experimental Mechanics, Vol. 5, No. 7, July 1965, pp. 193-226.

12. Coffin, L. F., Jr., "A Study of the Effects of Cyclic Thermal Stresses on a Ductile Metal," Transactions, American Society of Mechanical Engineers, Vol. 76, August 1954, pp. 931-950.

13. Robinson, E. L., "Effect of Temperature Variation on the Long-time Strength of Steels," Transactions, American Society of Mechanical Engineers, Vol. 74, 1952, pp. 777-781.

14. Hoffman, C. A., "Strengths and Failure Characteristics of AMS 5765A (S-816) Alloy in Direct Tensile Fatigue at Elevated Temperatures," Proceedings, American Society for Testing and Materials, Vol. 56, 1956, pp. 1063-1080.

15. Swindeman, R. W., in Proceedings, Joint International Conference on Creep, Institution of Mechanical Engineers, London, 1963, pp. 3-71 to 3-76.

16. Sheffler, K. D., and Doble, G. S., "Influence of Creep Damage on the Low Cycle Thermal-Mechanical Fatigue Behavior of Two Tantalum-Base Alloys," NASA CR-121001, National Aeronautics and Space Administration, May 1972.

17. Howes, M. A. H., "Thermal Fatigue Data on 15 Nickel- and Cobalt-Base Alloys," NASA CR-72738, National Aeronautics and Space Administration, May 1970.

18. Spera, D. A., Howes, M. A. H., and Bizon, P. T., "Thermal-Fatigue Resistance of 15 High-Temperature Alloys Determined by the Fluidized-Bed Technique," NASA TM X-52975, National Aeronautics and Space Administration, March 1971.

19. Manson, S. S., and Hirschberg, M. H., "Low Cycle Fatigue of Notched Specimens by Consideration of Crack Initiation and Propagation," NASA TN D-3146, National Aeronautics and Space Administration, June 1967.

20. Halford, G. R., "Cyclic Creep-Rupture Behavior of Three High-Temperature Alloys," NASA TN D-6309, National Aeronautics and Space Administration, May 1971.

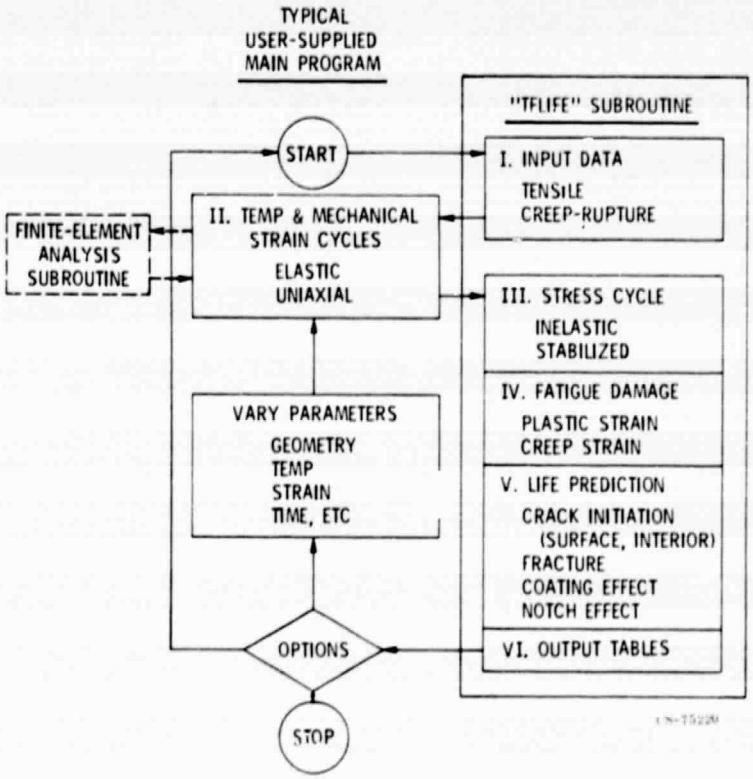

Figure 1. - Schematic diagram of computer program for predicting thermal fatigue life.

E-850

PRECEDING PAGE BLANK NOT FILMED

ORIGINAL PAGE IS
OF POOR QUALITY

PROBLEM 1.04

TABLE 2. PREDICTED CYCLIC LIVES AND DAMAGE FRACTIONS

FAILURE CRITERION		STRAIN CONC. FACTOR	CYCLES TO FAILURE	DAMAGE FRACTIONS	
				PLASTIC	CREEP
CRACK INITIATION	SURFACE	1.00	41	0.042	0.958
	INTERIOR	1.00	41	0.042	0.958
COMPLETE FRACTURE (THERMAL-MECHANICAL FATIGUE ONLY)		1.00	41	0.042	0.958
		2.15	36	0.167	0.833
		3.00	31	0.271	0.729

(a) Fatigue life and damage predictions. CS-75219

Figure 2. - Sample output tables (in-phase thermal-mechanical testing of the tantalum-base alloy T-111).

PROBLEM 1.04

TABLE 3. THERMAL, STRAIN, AND STRESS CYCLES

(A) HEATING HALF-CYCLE

TIME, MIN	TEMP, DEG K	STRAIN			STRESS, N/SQ CM
		MECH.	PLASTIC	CREEP	
0.000	478	-.009570	-.000000	0.000000	-56118
0.039	506	-.008622	-.000000		
0.078	535	-.007662	-		
0.117	563	-			
				0.002253	42962
			0.009365	0.002792	40846
		-.008740	0.009365	0.003317	38684
1.290	1421	0.009138	0.009365	0.003928	36739

(b) Thermal, strain, and stress cycles. CS-75223

Figure 2. - Continued.

PROBLEM 1.04

TABLE 4. MONOTONIC STRESS AND STRAIN PROPERTIES

TEMP, DEG K	YOUNG'S MODULUS, N/SQ CM	YIELD STRESS (.002), [1] N/SQ CM	ULTIMATE TENSILE STRESS, N/SQ CM	TENSILE DUCTILITY	POISSON'S RATIO	THERMAL EXPANSION FROM RT, PER DEG K
200	18.7E 06	56000	63500	0.800	0.265	6.05E-06
294	[illegible]	51000	60100	[illegible]		
539	18.1E 06	48075	[illegible]			
408	17.9E 06	[illegible]				
					0.280	7.09E-06
			49950	1.255	0.290	7.14E-06
		44300	17800	1.350	0.300	7.19E-06
1799	15.2E 06	12000	15000	1.450	0.316	7.25E-06

1 RATIO OF CYCLIC TO MONOTONIC YIELD AND ULTIMATE STRESSES = 1.43

(c) Monotonic stress and strain properties. CS-75225

Figure 2. - Continued.

PROBLEM 1.04

TABLE 5. MONOTONIC CREEP-RUPTURE BEHAVIOR

$LOG(Z) = A + B \cdot LOG(X) + C \cdot X + D \cdot X^2 + E \cdot Y$ $\qquad Z = T1$ OR TR

T1 = TIME TO 1 PCT CREEP, HR $\qquad$ TR = TIME TO RUPTURE, HR

CREEP RATE = $0.01/T1, HR^{-1}$ $\qquad$ X = STRESS/1000 N/SQ CM

$Y = (TEMP/1000\ K)^{BETA}$ $\qquad$ OR $\qquad$ LOG(TEMP/1000 K), IF BETA = 0

Z	A	B	C	D	E	BETA
T1	-9.198	-4.6670	0.00000	-.001569	23.791	-1.00
TR	-7.729	-4.6670	0.00000	-.001569	23.478	-1.00

(d) Monotonic creep-rupture behavior. CS-75218

Figure 2. - Concluded.

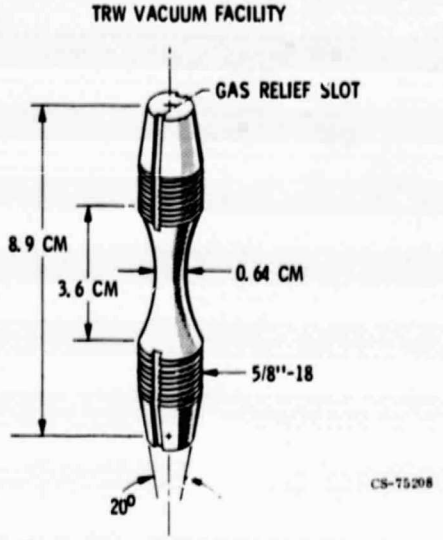

(a) Thermal-mechanical fatigue bar specimen (ref. 16).

Figure 3. - Geometry of specimens in sample problems.

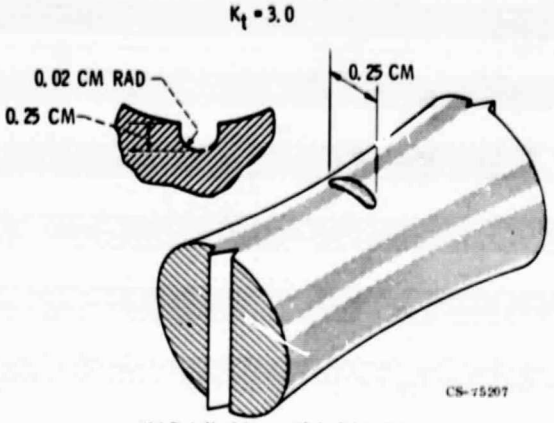

(b) Detail of tangential slot notch.

Figure 3. - Continued.

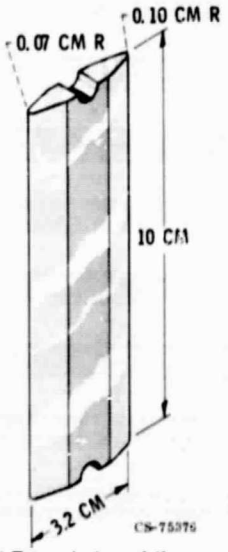

(c) Thermal-stress fatigue wedge specimen (refs. 17 and 18).

Figure 3. - Concluded.

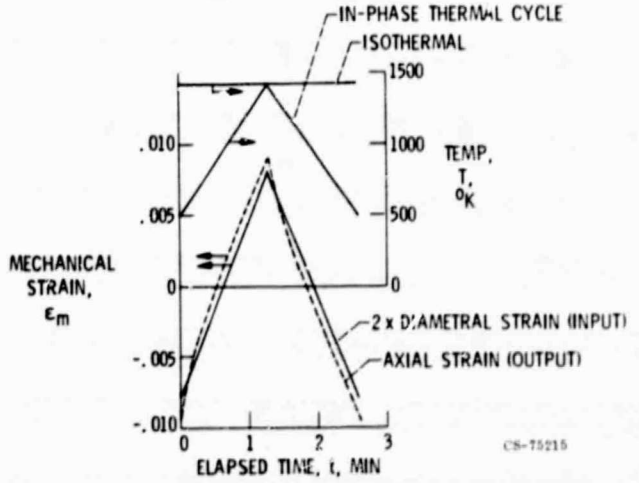

Figure 4. - Typical thermal and strain cycles applied during thermal-mechanical fatigue testing of the tantalum-base alloy T-111.

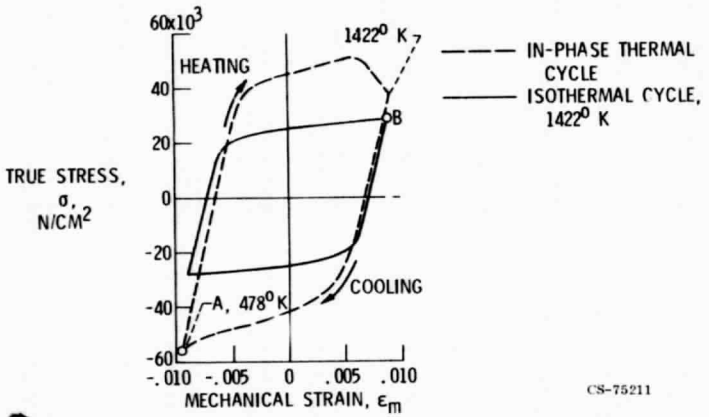

Figure 5. - Typical calculated stress-strain behavior during thermal-mechanical fatigue testing of the alloy T-111.

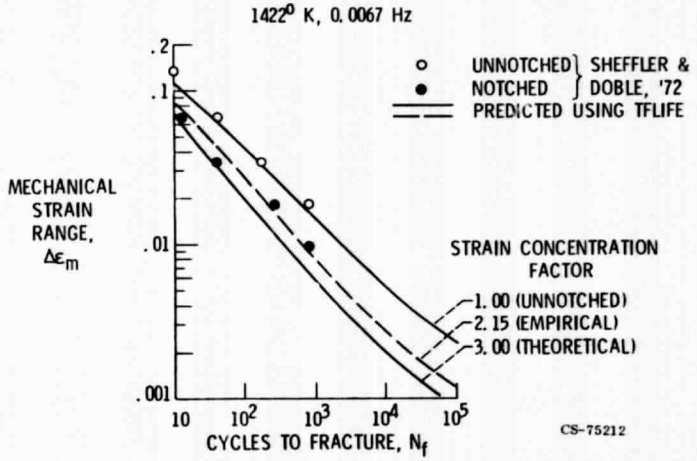

Figure 6. - Comparison of predicted and observed fatigue lives for isothermal cycling of the alloy T-111 in the unnotched and notched conditions (1422 K, 0.0067 Hz).

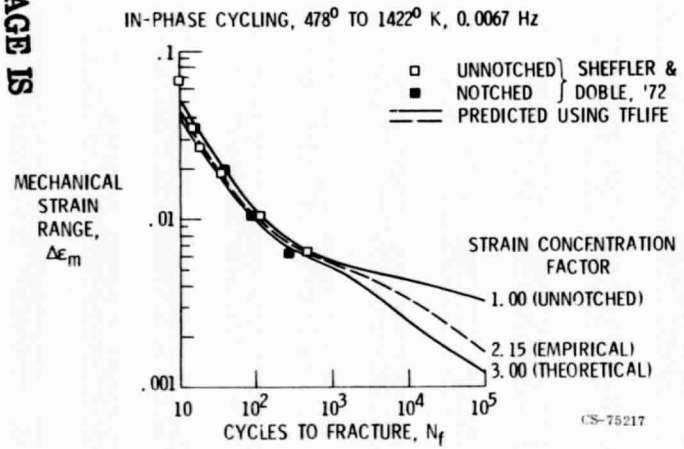

Figure 7. - Comparison of predicted and observed fatigue lives for in-phase thermal cycling of the alloy T-111 in the unnotched and notched conditions (478 K to 1422 K, 0.0067 Hz).

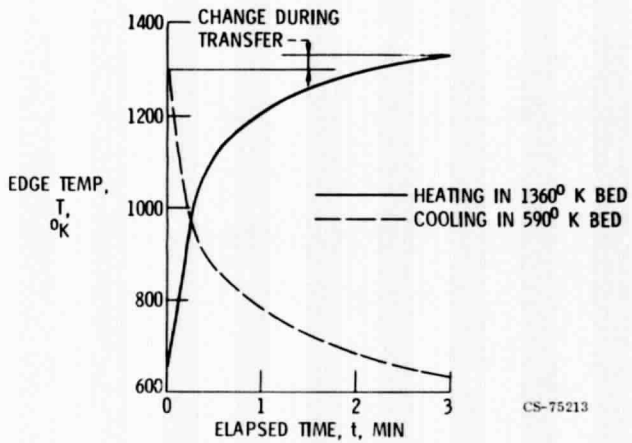

Figure 8. - Typical temperature transients at the edge of wedge specimens of the alloy B-1900 during thermal-stress fatigue testing.

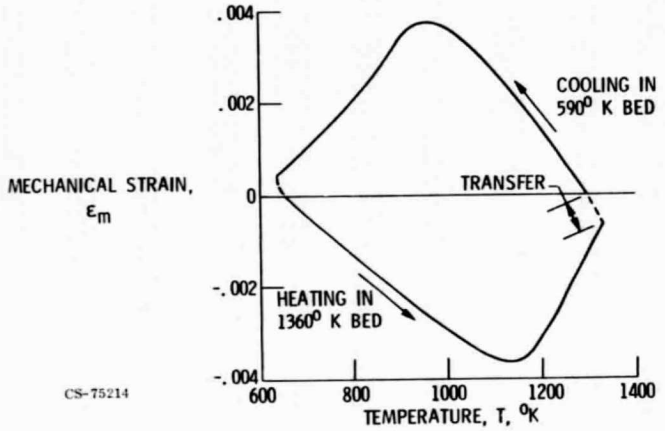

Figure 9. - Typical calculated strain-temperature behavior during thermal-stress fatigue testing of the alloy B-1900.

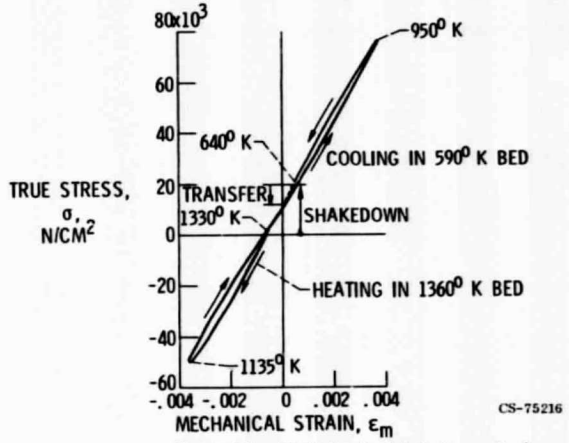

Figure 10. - Typical calculated stress-strain behavior during thermal-stress fatigue testing of the alloy B-1900.

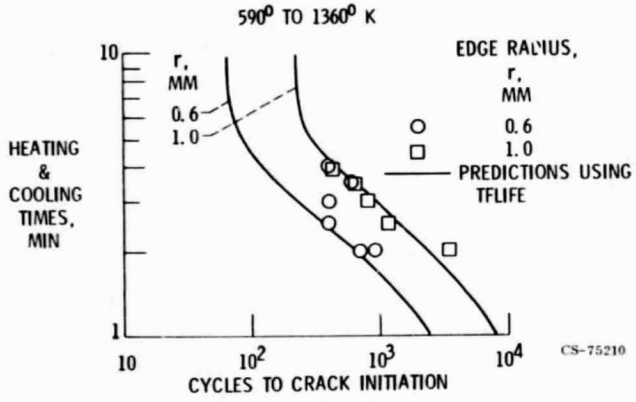

(a) Uncoated condition.

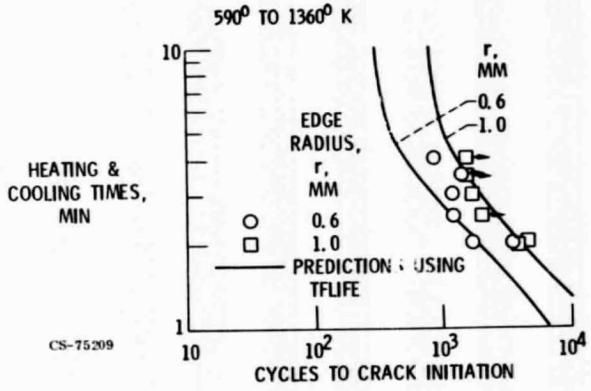

(b) Aluminide-coated conditions.

Figure 11. - Comparison of predicted and observed thermal-stress fatigue lives for the alloy B-1900 (wedge specimens tested in fluidized beds at 590 K and 1360 K; data from ref. 17).

Figure 11. - Concluded.